



Natural carbohydrate gums based hydrogels

Divya Balodhi, Khushbu, Sudhir G Warkar, Archana Rani & Rajinder K Gupta*
Department of Applied Chemistry, Delhi Technological University, Delhi, India

E-mail: rkg67ap@yahoo.com

Received 29 December 2020; accepted 24 March 2021

The future of good research lies in the search of innocuous material development, based primarily on natural resources. Keeping in this perspective, four different natural gums namely, Locust bean Gum, Gum Ghatti, Gum Tragacanth, and, Gum Acacia, are used to synthesize four different novel hydrogels via free radical polymerization method with sodium acrylate and acrylamide. The synthesis is evident with the help of characterization using TGA (Thermo Gravimetric Analysis), FTIR (Fourier Transform Infrared Spectroscopy), SEM (Scanning Electron Microscope), ^{13}C NMR (Nuclear Magnetic Resonance), and swelling studies in buffer solutions of pH 4, pH 7.4, pH 9.2, and, in distilled water. The synthesized hydrogels are potent enough in its potential utility in pharmaceuticals, drug delivery, tissue engineering as scaffolds that generally mimic human skin and in wound healing activity by incorporating the drug into it.

Keywords: Gum Acacia, Gum Ghatti, Hydrogels, Locust bean gum, Tragacanth

In the recent decades, prominent interest has been dedicated to the development of hydrogels which are three-dimensional crosslinked polymers possessing the ability to assimilate water-fluids in them and prevent its dissolution in water due to the presence of crosslinks present in them¹. The factors influencing hydrogels are temperature, pH, solvent composition, magnetic field, and ionic strength^{2,3}. Nowadays, most of the commercial hydrogels are being made of synthetic polymers, thus non-biodegradable and considered as contaminant due to their inappropriate disposal causing the alarming situation in the entire world. To uphold an eco-friendly environment, synthetic polymers have an immediate need to get replaced by natural ones as problems of plastic pollution, air pollution, global warming, ozone depletion is causing a threat to the environment as well as human health. However, it is imperative to utilize natural substances as raw materials for different applications to curtail environmental problems as with the time dramatic shift has been seen towards novel materials derived from them. Biopolymeric hydrogels have fascinated many sectors due to their biocompatibility and their harmless nature⁴. They have exhibited novel applications in the field of biomedical i.e. in drug delivery, wound healing, and in a tissue scaffold generation⁵. Their major feasibility has also been seen in the agriculture area as they have been explored as soil conditioners and even they act as a

mini reservoir that retains water and helps improving texture and fertility of soil^{6,7}. Presently, a lot of natural polymer-based hydrogels have been prepared using various biopolymers.

The focus of this research is on natural gum-based hydrogels, the reason being versatility of biopolymers, as significant improvements have been witnessed as it serves as a novel alternative over synthetic polymers. Technically, they have many advantages which makes it more favourable. They are environmentally friendly, green, biodegradable, renewable, and hence are compatible with nature. They are conveniently available and are generally low cost. They are non-toxic and can easily be modified by improving their characteristics as they possess a huge amount of structural diversities in them⁸.

Gum Tragacanth^{9,10} is a natural polysaccharide that usually consists of galacturonic acid, xylose, arabinose, galactose, and fucose in its chain. The presence of carboxylic and hydroxyl groups helps in reacting with the monomer and cross-linker¹¹⁻¹³. It is a very resourceful bio-polymer and contains two fraction mixture in its main chain, i.e. "tragacanthin", which usually dissipate to give a colloidal solution and the insoluble section, i.e. "bassorin", which usually has the potential to show swelling in an aqueous medium. The chemistry of GT allows it for the amalgamation of superabsorbent hydrogels¹⁴. Its potential utility is seen in the biomedical sector as reported by Singh *et al.* (2017) for wound healing

with the help of hydrogel dressing in which they have cross-linked GT with cotton fiber¹⁵.

Gum Ghatti is a natural polysaccharide and has drawn attraction due to its biocompatible, biodegradable, and non-toxic nature. Its main chain constituents are D-Galactose, D-Glucuronic acid, D-xylose, L-arabinose¹⁶. It is generally water-soluble and its plant belongs to the family *Combretaceae*. Its most frequent names are dhau, dhawa, raam, etc. It shows its occurrence in the mainly arid forests and it is generally glossy in texture^{17,18}. It consists of many salt constituents like calcium, potassium, magnesium, and sodium salt. GG based hydrogels have shown their application in pharmaceuticals, controlled drug delivery applications as reported where they have been developed as hydrogels by varying the concentration of crosslinker to the monomer by microwave radiation method¹⁹.

Gum Acacia is obtained as a gum exudate. It is composed of 1, 3-linked β -D-galactopyranosyl units, L-rhamnose, L-Arabinose, and D-glucuronic acid. It is generally water-soluble²⁰. They are generally found in the west of Africa to generally to the Indian peninsula. GA is the oldest natural gum and is generally recognized as safe (GRAS) and has shown

its potential application in the food industry and textile industry. It is also known for its gelling agent, stabilizer and also helps in the extension of shelf life of food. The major applications are seen in biosensors, drug delivery, and even in the agriculture area²¹. Locust Bean is a versatile biopolymer which has application in the food and pharma industry and even has potential use in tissue engineering, in implants²². It consists of 1,4 linked D-mannopyranosyl units in its main chain²³. It is generally obtained from seeds while the powder form is produced via milling of the endosperm. It is found in the geographical region of Asia, Africa, and even in South America is also referred to as carob bean gum which belongs to the *Fabaceae* family. The presence of galactose in its chain enhances its functionality and hence is easy to modify. Fig.1 represents the structure of all-natural gums²⁴.

The peer focus of this paper is on natural gums based hydrogels, their synthesis, evaluation of physical and chemical properties, and their comparative analysis. According to our literature survey, LB, GT, GG, and GA have never been used to the best of our knowledge with sodium acrylate (SA) as a monomer in hydrogel preparation.

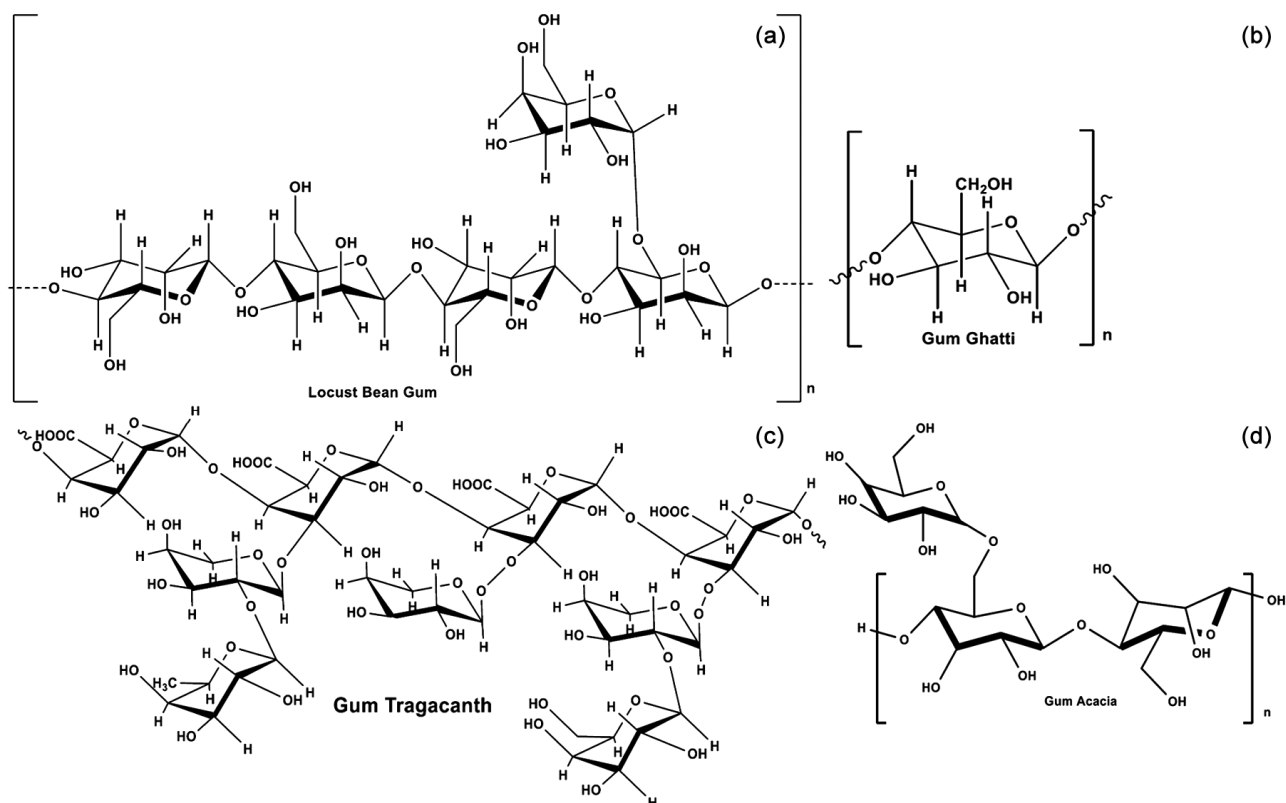


Fig.1 — Chemical Structures a) LB; b) GG; c) GT and d) GA

Experimental Section

Materials

Locust bean Gum (LG) (was purchased from Himedia Laboratories Pvt. Ltd, Mumbai, India), Tragacanth Gum (TG) (Loba Chemie Pvt. Ltd), Gum Acacia (GA) (Sigma Aldrich, USA), Gum Ghatti (GG) (CDH, New Delhi), Acrylic Acid (AA), (CDH New Delhi), Acrylamide (AM), (CDH, New Delhi), N, N'-methylene bis (acrylamide) (MBA), (CDH, New Delhi), Potassium persulfate (KPS), (Fischer Scientific, Mumbai), Sodium Hydroxide (Fischer Scientific, Mumbai) were used as such without further purification. Distilled water (DW) was used as a solvent in all the experiments.

Synthesis of Natural Gum Based Hydrogels

The hydrogels were synthesized using all four natural gums separately. In brief, all set of hydrogels was prepared by free radical polymerization

mechanism. All the reactions took place at 25°C. The hydrogels were prepared by dispersing the pre-fixed amount of natural gum, SA, acrylamide in 50 mL DW separately for all four gums. Afterward KPS and N,N'-MBA were added to the beakers to homogenize solution using a magnetic stirrer. After stirring for 2h, the mixture was transferred into test tubes and was allowed to cure at 60°C in a water bath. Then the cured hydrogels were sliced into thin discs and were washed using DW to remove unreacted monomers. Finally, these discs were air-dried at room temperature and further dried at 40°C for 3-4 days till constant weight was achieved in a hot air oven. Pictorial representation of the preparation method of the hydrogel is shown in Fig.2.

Swelling studies

Swelling studies were conducted using a buffer solution of pH (4, 7.4 and 9.2) and DW at room

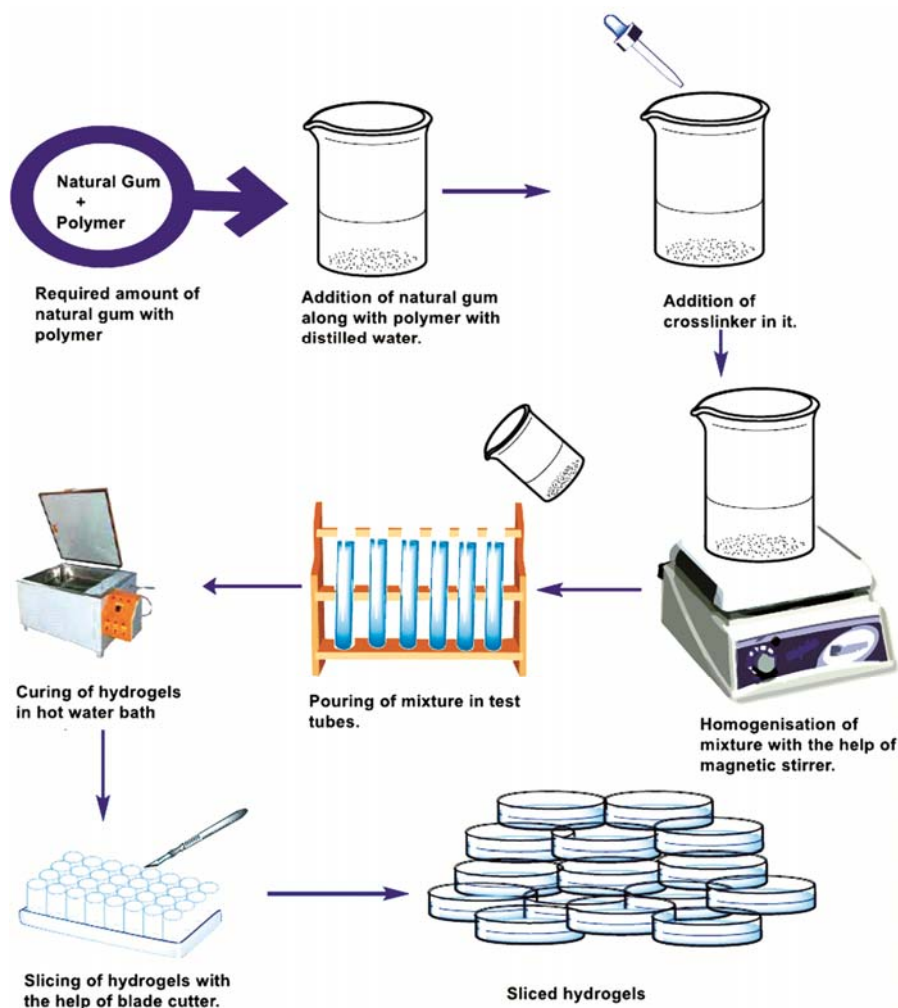


Fig.2 — Pictorial representation of hydrogel synthesis using natural gums.

temperature. The dried hydrogels of each gum were weighed and immersed in the buffer solution. Periodically, each swollen hydrogel was taken out and excess of water was wiped off using filter paper. The swelling index (SI) was calculated for each gum, according to the following formula (equation 1):

$$SI = (W_{SG} - W_{DG})/W_{SG} \quad \dots (1)$$

where, W_{SG} is the weight of swollen gel, and W_{DG} is the initial weight of dried gel. All the experiments were conducted in triplicates for all four hydrogels namely Locust bean hydrogel (LBH), Tragacanth gum hydrogel (TGH), Gum Ghatti hydrogel (GGH), Gum Acacia hydrogel (GAH). Table 1 Depicts the formulation of all gums along with its SI in DW.

Characterization

Structural studies of the natural gums were carried out using FTIR spectroscopy (Fourier Transform Infrared Spectroscopy), (by Perkin Elmer spectrum version 10.5.3) in ATIR mode. The TGA analysis was carried to study the thermal stability of the hydrogels with its gum derivative using a Perkin Elmer TGA analyzer in N_2 atmosphere. The temperature range was from ($25^\circ C$ to $900^\circ C$) with $10^\circ C/min$. XRD analysis was performed for each gum and its hydrogel using Bruker D8 ADVANCE X-ray diffractometer, angle ranging from 10° to 80° with an increment of 0.04° and scan speed of 0.5 Sec/step. SEM analysis was done for the examination of surface morphology of gums and hydrogels respectively, using JOEL JSM -6610LV. ^{13}C NMR was carried out for all four hydrogels and its derivative gums using model JOEL Resonance ECX-400.

Results and Discussions

Mechanism of formation of Hydrogels

Hydrogels were synthesized using KPS as initiator to produce free radicals. These sulfate-free radicals

attacks on the carboxyl groups of natural gums ($-COOH$) and became active in the reaction. The gums by donating hydroxyl groups ($-OH$) and formed covalent bonds with sodium acrylate and acrylamide causing propagation and hence polymerizing them into poly (sodium acrylate) and poly (acrylamide). Then cross-linker MBA, ($CH_2(CHCONHCH_2NHCOCH_2)$), was added to the reaction mixture of poly (sodium acrylate), poly (acrylamide), and natural gum. This resulted in the formation of the interpenetrating three-dimensional polymeric structure.

Swelling studies

The variation swelling indices (g/g) as a function of time (h) are studied for all four hydrogels and are compiled in the form of graphical representation in Fig.3. The swelling studies were conducted in DW at different pH (4, 7.4, 9.2). The swelling equilibrium for all the hydrogels were observed for about 28 (h). Interpretation of the SI in distinct solvents was recorded highest in the case of DW for all the hydrogels, which are 215 g/g, 171 g/g, 168 g/g, 203 g/g for LBH, GGH, TGH and GAH respectively. Interestingly, all four hydrogels showed a similar pattern of solvent absorption where SI tends to increase from (pH 4 to 6) and then decrease and further increasing to pH 8²⁵. For LBH, at pH 4, SI was 25 g/g followed by pH 7.4 in which SI was observed to be 18 g/g whereas, at pH 9.2, it was 43 g/g. Similarly, for GGH at pH 4 it was 27 g/g, at 7.4 it was 19 g/g and at pH 9.2 it was observed as 41 g/g. For TGH, the values of SI for pH 4, pH 7.4, pH 9.2 were 24 g/g, 17 g/g and 37 g/g and respectively. For GAH, the SI for pH 4, pH 7.4, pH 9.2 was observed as 27 g/g, 16 g/g, and 40 g/g (Table 2). According to the above evaluation, LBH was observed to have shown maximum SI in DW as compared to others. The increase in transition of swelling from pH 4 to pH 6 could be attributed to electrostatic repulsion of the

Table 1 — Formulation of all four natural gum-based hydrogel along with their Swelling Index (SI).

Gums used	Gums	Acrylic acid	NaOH	Acyl-amide	MBA	KPS/DW (g/mL)	Maximum SI
(LB)	0.5 g	5 mL	3.2g	5 g	60 mg	0.05/10	215 g/g
(GG)	0.5 g	5 mL	3.2g	5 g	60 mg	0.05/10	171 g/g
(TG)	0.5 g	5 mL	3.2g	5 g	60 mg	0.05/10	168 g/g
(GA)	0.5 g	5 mL	3.2g	5 g	60 mg	0.05/10	203 g/g

Table 2 — Swelling Index of all four natural gum-based hydrogels w.r.t the media used.

Hydrogels	Distilled water (g/g)	pH=4 (g/g)	pH=7.4 (g/g)	pH=9.2 (g/g)
(LBH)	215	25	18	43
(GGH)	171	27	19	41
(TGH)	168	24	17	37
(GAH)	203	27	16	40

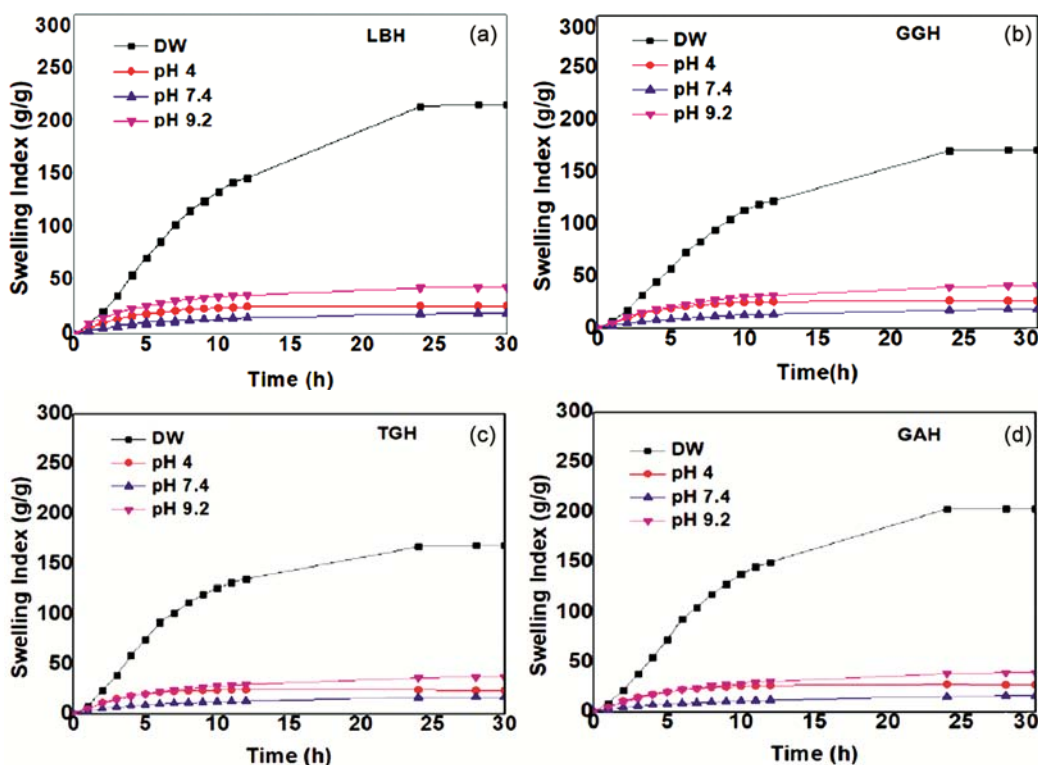


Fig.3 — Dynamic swelling studies a)LBH; b)GGH; c)TGH and d)GAH

hydrogel which results in drastic swelling at this pH range. Whereas, swelling tends to decrease in alkaline medium which may be due to the presence of excess sodium in the media, which results in shielding carboxylate anions ($-\text{COO}^-$) present in the hydrogels which might prevent anion-anion repulsion between them²³. Again transition in SI is seen at higher pH , which is at 9.2 where the hydrogels show drastic swelling as compared to pH 7.4 due to conversion of ($-\text{COOH}$) groups into ($-\text{COO}^-$) and causing electrostatic repulsion between them and dissociating hydrogen bonds²⁴.

Characterization

FTIR Spectroscopy (Fourier Transform Infrared Spectroscopy)

The FTIR analysis for all gums and their hydrogels is shown in Fig.4. In Fig.4a the peak at 3450 cm^{-1} emphasized the hydroxyl group for LB responsible for hydrogen bonding in the gum. The peaks at 2900 cm^{-1} and 1384 cm^{-1} are attributed to C-H stretching whereas peak at 1145 cm^{-1} is due to -OH bending. For LBH, the peak for -OH group in LB is shifted to 3334 cm^{-1} and the intensity is decreased depicting crosslinking in the hydrogel as compared to gum. The peak at 1663 cm^{-1} (C=O), 1033 cm^{-1} (C-O-C) showed the presence of the amide linkage due to poly (acrylamide), and it

was evident that the reaction between the monomer and crosslinker had taken place²⁵. The peak at 3433 cm^{-1} is for the hydroxyl group in GG (Fig.4b). Similarly, peaks at 2992 cm^{-1} and 1102 cm^{-1} are due to C-H stretching and C-O bending. Further peaks at 1551 cm^{-1} and 1626 cm^{-1} are observed due to -COOH symmetric and asymmetric vibration. Similarly, GGH showed the presence of -OH group at peak 3338 cm^{-1} . The strong peak at 1798 cm^{-1} was observed, which attributed to absorption shown due to the linking of poly (sodium acrylate) to gum depicting C=O functional group. In the FTIR spectra of GT shown in Fig.4c, the absorption peak for -OH group was also observed at 3423 cm^{-1} . The peaks observed at 1625 cm^{-1} and 1743 cm^{-1} are dedicated to -COOH and -C=O groups respectively. The graph shown for GTH where the -OH peak is observed at 3423 cm^{-1} . The peaks at 1720 cm^{-1} , 1553 cm^{-1} are due to C=O, and -COO asymmetric vibrations and assured the crosslinking of monomer on natural polysaccharide²⁶. In Figure 4d, GA also showed -OH functional group having a peak at 3398 cm^{-1} . The peaks from ($1000-1074\text{ cm}^{-1}$) showed C-O-C symmetric and asymmetric vibration, thus, authenticated the functional group present in the gum that has been reported. GAH also showed hydroxyl group, but with the drop in its

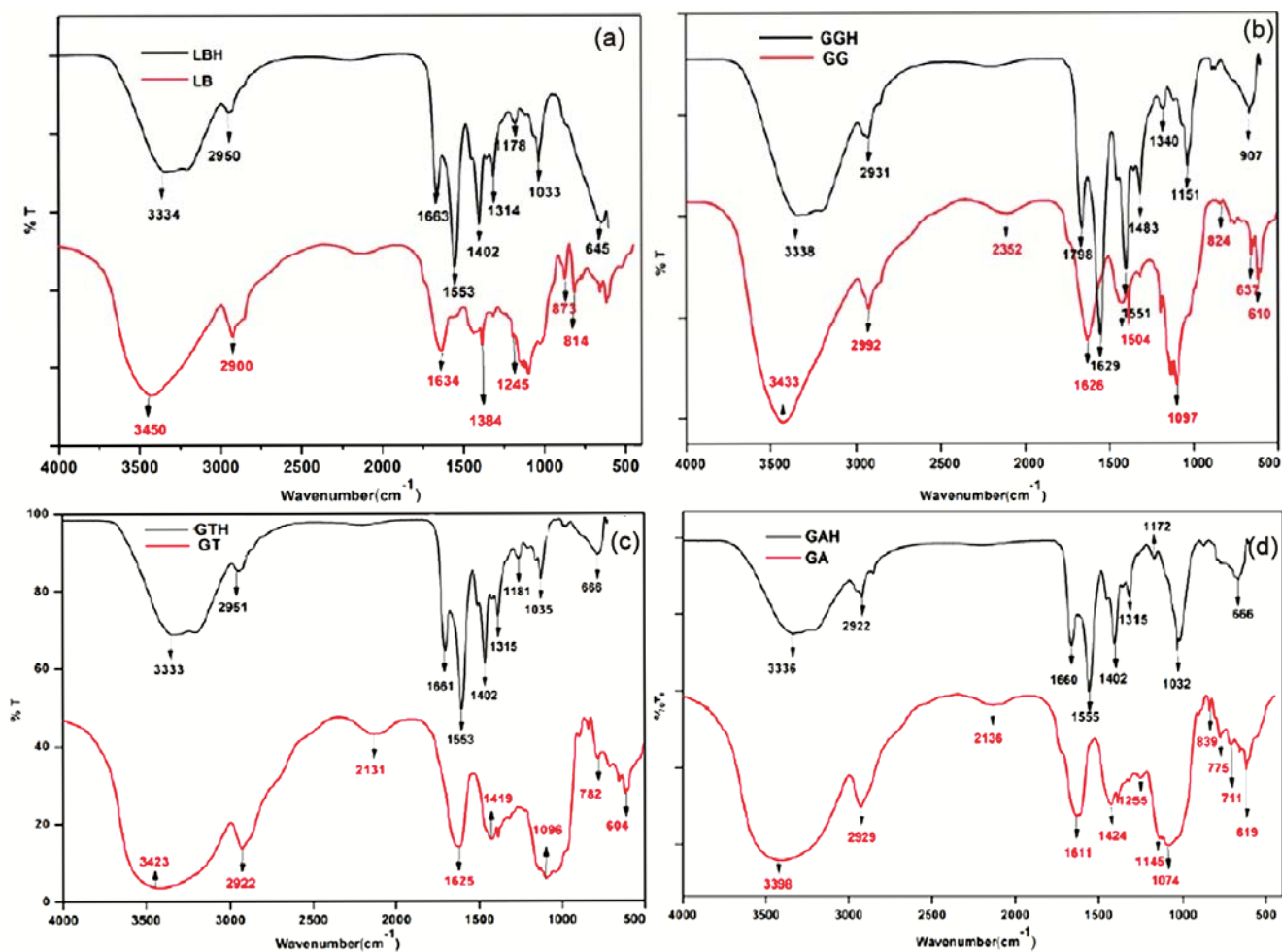


Fig.4 — FTIR Spectra of gums along with their hydrogels a) LB & LBH b) GG & GGH c) GT & GTH d) GA & GAH

intensity as interpreted by comparative analysis with the gum i.e. 3336 cm^{-1} . Amide linkage was seen at 1660 cm^{-1} (C=O) and 1555 cm^{-1} (C-O) asymmetric stretching was observed, which justified the presence of poly (sodium acrylate) and poly (acrylamide) in the hydrogel²⁷.

Thermal analysis

TGA graphs of all hydrogels with their gums are displayed in Fig.5. In LB, weight loss was 1.83% in the initial period ($120\text{--}236^\circ\text{C}$) which could be associated due to loss of moisture from the gum. The second phase ($236\text{--}347^\circ\text{C}$) of weight loss was 56.37% that might be due to the degradation of the main chain constituents. The third transition was seen to have a weight loss of 18.88 % at ($347\text{--}772^\circ\text{C}$) which could be responsible due to further decomposition of glycosidic linkages in it²⁶. In LBH, the initial decomposition occurred at ($202\text{--}446^\circ\text{C}$) with a weight

loss of 38.98% due to entrapped water in it. The second transition ($446\text{--}513^\circ\text{C}$) shows 9.76% weight loss & the third phase ($513\text{--}772^\circ\text{C}$) weight loss% was off 11.88% because of degradation of polymeric chains of cross-linked networks. Hence, in comparison of LBH to LB, LBH seems to have more thermal stability as residual mass left at 722°C was 31 % and 13 % respectively from which it is interpreted that modification of gum has led to increase in its degradation temperature. Similarly, for GG two-phase decomposition was observed first in ($223\text{--}329^\circ\text{C}$) and second at ($329\text{--}772^\circ\text{C}$) with a weight loss % of 42.64 & 26.51 % due to moisture removal and degradation of biopolymer. In GGH, a three-phase decomposition pattern was observed as for the initial stage ($184\text{--}425^\circ\text{C}$), second stage ($425\text{--}524^\circ\text{C}$), third stage ($524\text{--}772^\circ\text{C}$) that was 33.21, 16.42 and 11.6 weight loss%. The residual mass leftover at the final decomposition temperature for both GG and GGH was 14.14 and

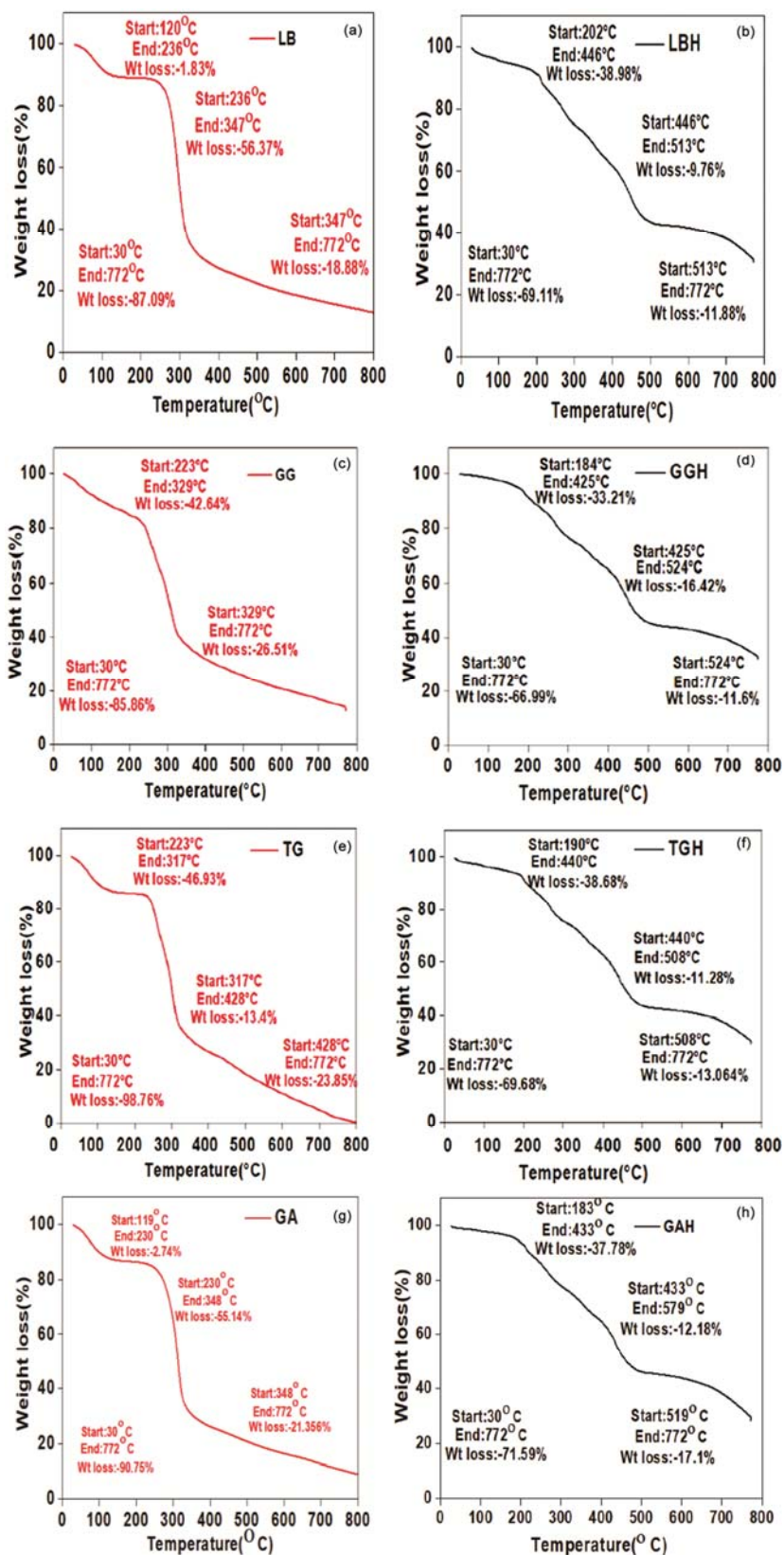


Fig.5 — Depicting TGA analysis of a) LB; b) LBH; c) GG; d) GGH; e) GT; f) GTH; g) GA and h) GAH

33.01%, which clearly illustrated the improved thermal stability in case of GGH¹⁹. For TG and TGH three-phase decomposition occurred. For TG, it was for an initial period (223-317°C), the second stage (317-428°C), the third stage (428-772) depicted the weight loss % that was 46.93%, 13.40%, and 23.85%, respectively which could be due to water removal at the initial stage and the degradation of bio-polymer at second and third transition¹⁵. In TGH, the initial period (190-440°C), the second stage (440-508°C), the third stage (508-772°C) displayed weight loss % that were 38.68%, 11.28% and lastly 13.06%. The residual mass left at the final temperature (722°C) for Gum and hydrogel was approximately 1% and 30% respectively from which it is evident that alteration in the arrangement of polymeric networks has enhanced the thermal stability of the modified gum. In GA, three-phase decomposition was observed from (119-230°C) with a weight loss of 2.74% due to (-OH) hydroxyl group removal. The second transition was from (230-348°C) which portrayed 55.14% weight loss which was due to degradation in the main chain. The third decomposition observed was from (348-772°C) with a 21.35% weight loss. Similarly for GAH, the initial stage was from (183-433°C), the second stage (433-579°C), followed by the third stage

(519-772°C) which illustrated weight loss of 37.78 % due to moisture removal, 12.18% in the second phase and 17.10% in the third phase respectively due to disruption in cross-linked polymer network due to degradation with temperature respectively²⁷. The residual mass left at the final temperature was recorded more than 19.16 % for GAH than GA, which validated more thermal stability of GAH over GA. These observations clearly showed that thermal stability has increased in the case of all the hydrogels as compared with their native natural gums.

XRD analysis

XRD is usually done for the analysis of crystalline, semi-crystalline and amorphous nature of the material. The XRD analysis for all the gums and their hydrogels were conducted and shown in Fig.6. Indigenous gums have shown sharper peaks as compared with their respective hydrogels indicating a decrease in the crystalline nature of the polymeric structures on the formation of hydrogels from their gums. The XRD graph of LB and LBH (shown in Fig. 6a), a sharp peak observed at 19.08° for LB converts to a broadened peak at 23.88° for LBH which depicted the amorphous nature of LBH due to formation of amorphous linkages²⁵. The XRD graph shown in Fig.6b for GG

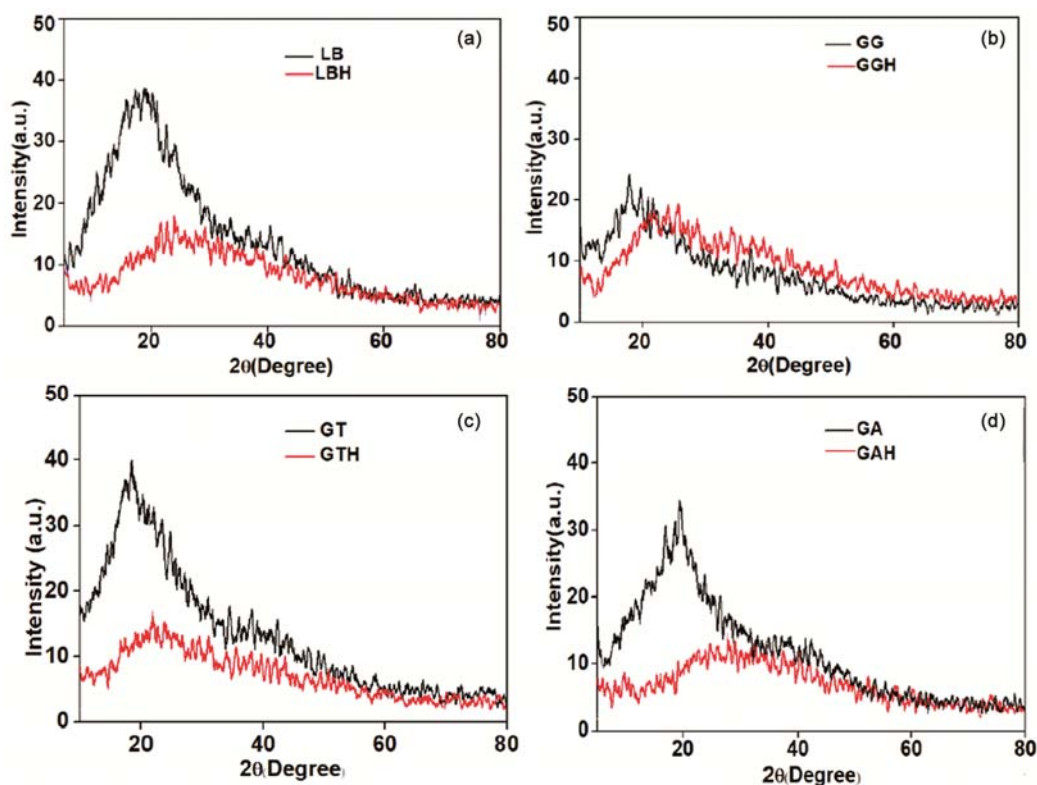


Fig.6 — Representation of XRD plot a) LB & LBH; b) GG & GGH; c) GT & GTH and d) GA & GAH.

showed a strong peak at 19.18° which indicated its crystallinity as reported in the literature¹⁶. The deviation in the peak of GGH was seen after crosslinking that affirmed its amorphous nature which might be due to disorientation in the structural arrangement of the crosslinked hydrogel at 24.11° (Ref.30). Similarly in Fig.6c for TGH, the peak at 21.72° was observed that showed modification in peak due to the formation of new networks, which reduced the interaction among TG chains which resulted in

declining of semi-crystalline nature when compared to its native gum¹². The XRD graph shown in Fig.7d for GA, the peak at 19.36° shifted to 27.88° for GAH (due to the modification of the GA in GAH on co-polymerization and crosslinking)³¹.

Scanning Electron Microscopy

SEM analysis of each hydrogel (LBH, GGH, GTH, GAH) and their gum (LB, GG, GA, GT) has been done and is presented in Fig.7. As shown in the figure

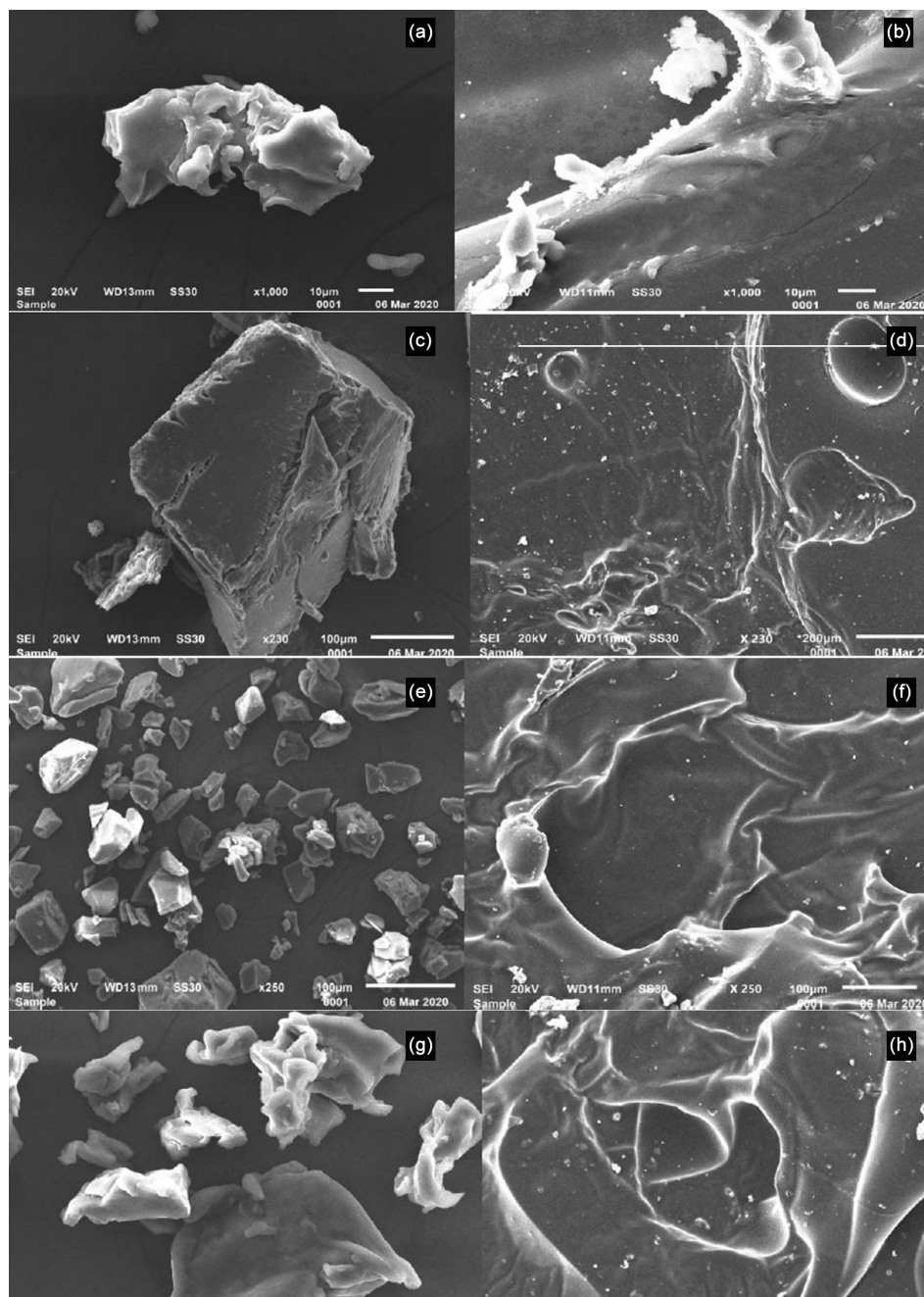


Fig.7 — Surface morphology of each gum with its respective hydrogel a) LB; b) LBH; c) GG; d) GGH; e) GT; f) GTH; g) GA and h) GAH

super absorbent hydrogels were having a porous morphology with a rough surface which seemed to be responsible for its swelling behaviour as it allowed more liquid to penetrate in these voids. These pores were associated with higher swelling as they allowed direct diffusion of liquid in the crosslinked network. The gums were compact and having a non-porous

surface which indicates that gum has been modified, forming interpenetrating networks due to the presence of cross-linking in them.

Solid-state NMR

Solid-state ^{13}C NMR of gum and their hydrogel is depicted below in Fig.8. LB showed a peak at δ

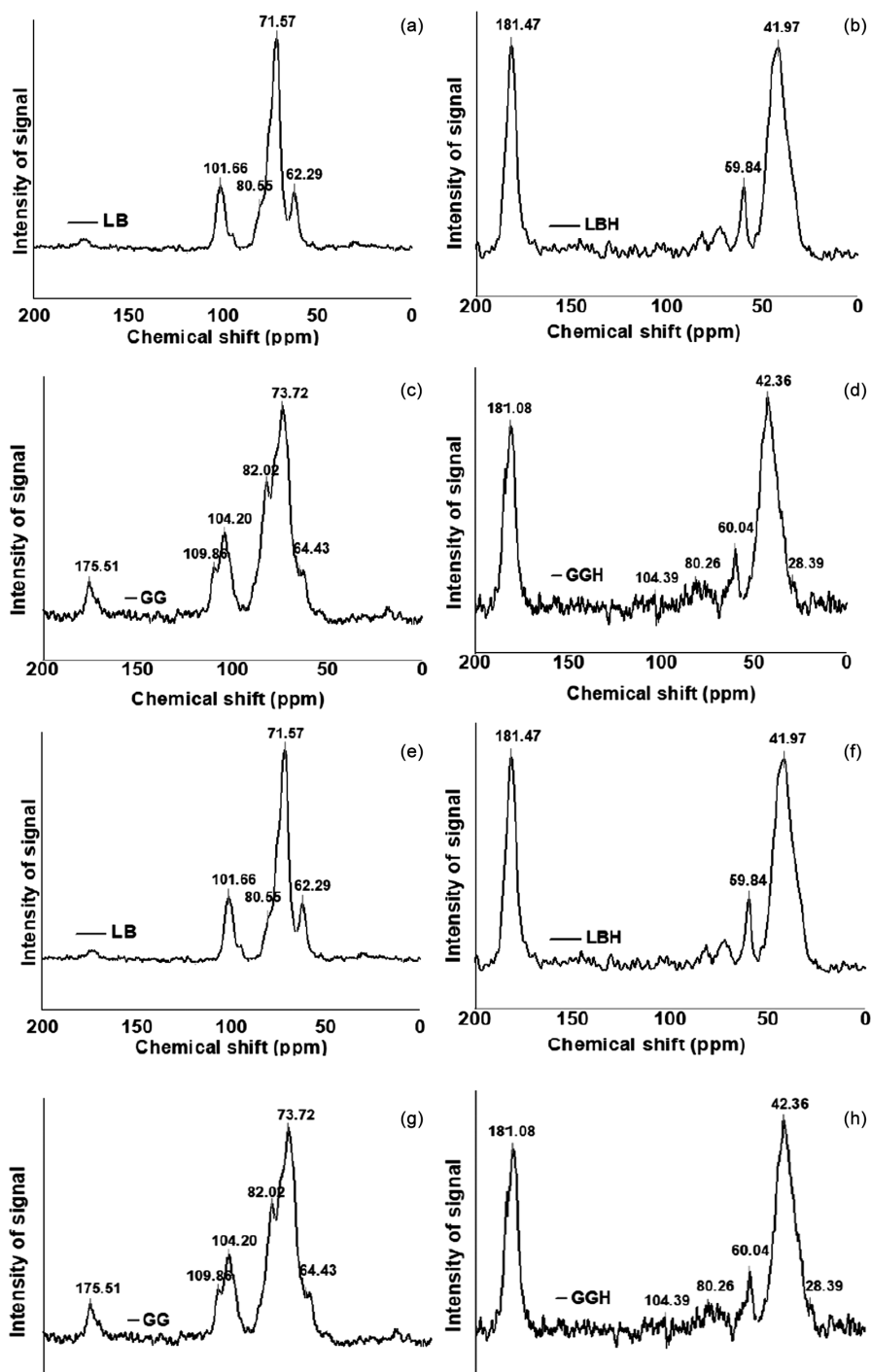


Fig.8 — ^{13}C NMR Spectrum of a) LB; b) LBH; c) GG; d) GGH; e) TG; f) TGH; g) GA and h) GAH

=101.66 ppm, which was due to the mannose unit of C₁. The signal peak at $\delta = 80.55$ ppm observed, which represented the C₄ mannan whereas C₆ Carbon of LB mannose unit showed a peak at $\delta = 62.29$ ppm²⁸. The hydrogel synthesized i.e. LBH showed a new signal peak at $\delta = 181.47$ ppm due to the carboxylate group (-COO) of poly(sodium acrylate). The peak at $\delta = 59.45$ ppm was for the C₆ mannan carbon atom of gum. Lastly, the peak at $\delta = 41.97$ ppm showed the presence of methylene carbon which was due to crosslinker present in it²⁹. The peaks clearly showed the modification of gum in hydrogels. For GG NMR spectrum, a peak observed at $\delta = 175.51$ ppm due to the presence of acid D-glucuronic acid, peak at $\delta = 104.20$ ppm due to presence of cyclic saccharides in its chain, peak at $\delta = 64.43$ ppm due to existence of -CH₂-OH group in its chain which confirmed the structure of gum³⁰. For GGH, the peaks observed at $\delta = 181.05$ ppm due to -COO group present due to poly (sodium acrylate). The peaks at $\delta = 104.39$ ppm, $\delta = 80.26$ ppm & $\delta = 60.04$ ppm confirmed hydrogel synthesis. The new peak at $\delta = 42.36$ ppm was due to the introduction of crosslinks in the hydrogel due to N, N-MBA. NMR spectrum of TG, a peak at $\delta = 104.10$ ppm due to cyclic saccharides present in its main chain, peak at $\delta = 81.53$ ppm for a C₃ carbon atom and a peak $\delta = 63.07$ depicted -CH₂-OH group in the natural gum³¹. Similarly, NMR peaks of TGH at $\delta = 181.37$ ppm, $\delta = 60.53$ ppm, $\delta = 42.06$ ppm confirmed the synthesis of the hydrogel by crosslinking poly (sodium acrylate) on TG with the help of N, N-MBA. For GA, a peak observed at $\delta = 176.20$ ppm for -COOH group present in its backbone, peak at $\delta = 104.20$ ppm for the presence of pyranose cyclic ring of an anomeric carbon atom of GA. A signal at $\delta = 72.25$ ppm depicted (-CH-OH) group and a peak $\delta = 62.75$ ppm due to CH₂OH present in the gum²⁷. In the crosslinked hydrogel i.e. GAH the peak was observed at $\delta = 181.47$ ppm, which was due to the presence of poly(sodium acrylate). The peaks at $\delta = 91.91$ ppm & $\delta = 81.73$ ppm confirmed the structure of GA present in hydrogel. A new peak was observed at $\delta = 41.28$ ppm, which was due to N, N-MBA. Hence, based on the ¹³C NMR data it is quite evident that all gums have been converted into super absorbent hydrogels in each case.

Conclusion

Natural Gum based hydrogels have shown their major utility in many areas due to their bio-

compatible, toxic, and eco-friendly nature. The produced hydrogels along with their gum were analyzed using TGA, SEM, XRD, ¹³C NMR, and swelling studies, and from this analysis, it is evident that gums have been modified into interpenetrating 3-D Networks. All hydrogels have been synthesized with the help of their native gums, which resulted in a crosslinked structure that can infuse a huge amount of water in its pores. SI was found to be maximum for LBH, in DW followed by GAH, GGH, and GTH respectively. Thermal stability also tends to increase as compared to their native gum. GGH, out of all had the highest degradation temperature due to leftover residual mass at 772°C that has a weight loss of 33.01 %, followed by LBH at 31 %, TGH at 30 %, and GAH at 28.41 %. The FTIR spectrum and ¹³C NMR helped in revealing the functional groups present in the gum and hydrogel hence confirmed the synthesis of the hydrogel. XRD analysis helped in interpreting the sharp peaks of gums which were due to semi-crystalline nature which was further altered to broad peaks showing amorphous nature due to modification of gums in crosslinked gel in which most of the alteration was seen in GAH that was 27.88° followed by GGH in 24.11°, LBH at 23.88° and TGH at 21.72°. SEM analysis helped in determining pores size, which was visible and helped in depicting surface morphology of gum and hydrogels. All four hydrogels synthesized using natural gums have shown the ability for water absorption due to their pores in their surface. SEM analysis helped in revealing surface morphology of hydrogel that was found to be porous when compared to the gums, which further helped in the swelling, study assessment that resulted in the assimilation of fluid into voids and hence confirmed the amalgamation of hydrogel's. More exclusive studies will help in understanding of hydrogel, which will absolutely upswing its competency in the ensuing years in diversified areas including biomedical, pharmaceutical and agricultural sectors.

Conflicts of Interest

There are no conflicts to be declared.

Acknowledgement

The authors are thankful to Delhi Technological University for their financial support, Delhi University (SEM), and IISC Bangalore (NMR) for their support in our research.

References

- 1 Akhtar M F, Hanif M & Ranjha N M, *Saudi Pharm J*, 24 (2016) 554.
- 2 Fallon M, Halligan S, Pezzoli R, Geever L & Higginbotham C, *Gels*, 5 (2019) 1.
- 3 Zhao Y, Kang J & Tan T, *Polymer (Guildf)*, 47 (2006) 7702.
- 4 Khushbu & Warkar S G, *Eur Polym J*, 140 (2020) 110042.
- 5 Bahram M, Mohseni N & Moghtader M, *Emerging Concepts in Analysis and Application of Hydrogels* (2016) 9.
- 6 Singh B, Sharma D K, Negi S & Dhiman, A *Int J Plast Technol*, 19 (2015) 263.
- 7 Behera S & Mahanwar P A, *Polym Technol Mater*, 59 (2020) 341.
- 8 Guilherme M R, *Eur Polym J*, 72 (2015) 365.
- 9 Nagaraja K, Rao K M, Reddy G V & Rao K S V K, *Int J Biol Macromol*, 174 (2021) 502.
- 10 Jahanban-Esfahlan R, *J Mater Res*, 1 (2021) 1.
- 11 Yang Z, Peng H, Wang W & Liu T, *J Appl Polym Sci*, 116 (2010) 2658.
- 12 Xie A J, Zhu C Y & Liu H M, *MOJ Food Process Technol*, 4 (2017) 192.
- 13 Gröbbl M, Harrison S, Kaml I & Kenndler E J, *Chromatogr A*, 1077 (2005) 80.
- 14 Farmer T J, Comerford J W, Pellis A & Robert T, *Polym Int*, 67 (2018) 775.
- 15 Singh B, Varshney L, Francis S & Rajneesh, *Radiat Phys Chem*, 135 (2017) 94.
- 16 Deshmukh A S, Setty C M, Badiger A M & Muralikrishna K S *Carbohydr Polym*, 87 (2012) 980.
- 17 Rani P, Sen G, Mishra S & Jha U, *Carbohydr Polym*, 89 (2012) 275.
- 18 Aspinall G O, Hirst E L & Wickstrom A, *J Chem Soc*, 1160 (1955).
- 19 Pal P, Singh S K, Mishra S, Pandey J P & Sen G, *Carbohydr Polym*, 222 (2019) 114979.
- 20 Shirwaikar A, Shirwaikar A, Prabhu S & Kumar G, *Indian J Pharm Sci*, 70 (2008) 415.
- 21 Patel S & Goyal A, *Int J Food Prop*, 18 (2015) 986.
- 22 Prajapati V D, Jani G K, Moradiya N G, Randeria N P & Nagar B J, *Carbohydr Polym*, 94 (2013) 814.
- 23 Dea I C M & Morrison A, *Adv Carbohydr Chem Biochem*, 31 (1975) 241.
- 24 Ahmad S, Ahmad M, Manzoor K, Purwar R & Ikram S, *Int J Biol Macromol*, 136 (2019) 870.
- 25 Mohamed S F, Mahmoud G A & Taleb M F A, *Monatshefte Fur Chem*, 144 (2013) 129.
- 26 Zauro S A & Vishalakshi B, *Indian J Adv Chem Sci*, 00 (2016) 88.
- 27 Singh B, Sharma S & Dhiman A, *Carbohydr Polym*, 165 (2017) 294.
- 28 Kaity S & Ghosh A, *Ind Eng Chem Res*, 52 (2013) 10033.
- 29 Candau F, Zekhnini Z & Heatley F, *Macromolecules*, 19 (1986) 1895.
- 30 Pal P, Suman S, Verma A, Pandey J P & Sen G, *Colloids Surfaces A Physicochem Eng Asp*, 555 (2018) 699.
- 31 Singh B, Varshney L, Francis S & Rajneesh, *Int J Biol Macromol*, 88 (2016) 586.